ORIGINAL RESEARCH

Toll-Like Receptor 9 Plays a Pivotal Role in Angiotensin II–Induced Atherosclerosis

Daiju Fukuda, MD, PhD;* Sachiko Nishimoto, PhD;* Kunduziayi Aini, MD; Atsushi Tanaka, MD, PhD; Tsuyoshi Nishiguchi, MD, PhD; Joo-ri Kim-Kaneyama, PhD; Xiao-Feng Lei, PhD; Kiyoshi Masuda, MD, PhD; Takuya Naruto, PhD; Kimie Tanaka, MD, PhD; Yasutomi Higashikuni, MD, PhD; Yoichiro Hirata, MD, PhD; Shusuke Yagi, MD, PhD; Kenya Kusunose, MD, PhD; Hirotsugu Yamada, MD, PhD; Takeshi Soeki, MD, PhD; Issei Imoto, MD, PhD; Takashi Akasaka, MD, PhD; Michio Shimabukuro, MD, PhD; Masataka Sata, MD, PhD

***Background*—**Toll-like receptor (TLR) 9 recognizes bacterial DNA, activating innate immunity, whereas it also provokes inflammation in response to fragmented DNA released from mammalian cells. We investigated whether TLR9 contributes to the development of vascular inflammation and atherogenesis using apolipoprotein E–deficient ($Apoe^{-/-}$) mice.

Methods and Results*—Tlr9*-deficient $Apoe^{-/-}$ ($Tlr9^{-/-}Apoe^{-/-}$) mice and $Apoe^{-/-}$ mice on a Western-type diet received subcutaneous angiotensin II infusion (1000 ng/kg per minute) for 28 days. Angiotensin II increased the plasma level of double-stranded DNA, an endogenous ligand of TLR9, in these mice. Genetic deletion or pharmacologic blockade of TLR9 in angiotensin II–infused $Apoe^{-/-}$ mice attenuated atherogenesis in the aortic arch ($P<0.05$), reduced the accumulation of lipid and macrophages in atherosclerotic plaques, and decreased RNA expression of inflammatory molecules in the aorta with no alteration of metabolic parameters. On the other hand, restoration of TLR9 in bone marrow in $Tlr9^{-/-}Apoe^{-/-}$ mice promoted atherogenesis in the aortic arch ($P<0.05$). A TLR9 agonist markedly promoted proinflammatory activation of $Apoe^{-/-}$ macrophages, partially through p38 mitogen-activated protein kinase signaling. In addition, genomic DNA extracted from macrophages promoted inflammatory molecule expression more effectively in $Apoe^{-/-}$ macrophages than in $Tlr9^{-/-}Apoe^{-/-}$ macrophages. Furthermore, in humans, circulating double-stranded DNA in the coronary artery positively correlated with inflammatory features of coronary plaques determined by optical coherence tomography in patients with acute myocardial infarction ($P<0.05$).

***Conclusions*—**TLR9 plays a pivotal role in the development of vascular inflammation and atherogenesis through proinflammatory activation of macrophages. TLR9 may serve as a potential therapeutic target for atherosclerosis. **(*J Am Heart Assoc*. 2019;8: e010860. DOI: 10.1161/JAHA.118.010860.)**

Key Words: atherosclerosis • inflammation • macrophage • Toll-like receptor 9 • vascular inflammation

Chronic inflammation in the vasculature causes atherosclerosis.[1] Although multifactorial in etiology, accumulating evidence indicates that the innate immune system plays a role in the development of vascular inflammation.[2] Immune cells such as macrophages recognize structures of pathogens through Toll-like receptors (TLRs), a family of pattern recognition receptors, and activate the innate immune system for self-defense.[3] On the other hand, recent studies have revealed that macrophages can also recognize molecules derived from damaged or dead host cells as endogenous ligands though TLRs, leading to the development of chronic sterile inflammation.[4,5] In fact, activation of

From the Departments of Cardiovascular Medicine (D.F., S.N., K.A., S.Y., K.K., T.S., M. Sata), Cardio-Diabetes Medicine (D.F., M. Shimabukuro), Human Genetics (K.M., T. Naruto, I.I.), and Community Medicine for Cardiology (H.Y.), Tokushima University Graduate School of Biomedical Sciences, Tokushima, Japan; Department of Cardiovascular Medicine, Wakayama Medical University, Wakayama, Japan (A.T., T. Nishiguchi, T.A.); Department of Biochemistry, Showa University School of Medicine, Tokyo, Japan (J.-r.K.-K., X.-F.L.); Division for Health Service Promotion (K.T.) and Department of Cardiovascular Medicine (Y. Higashikuni), The University of Tokyo, Japan; Department of Pediatrics, The University of Tokyo Hospital, Tokyo, Japan (Y. Hirata); Department of Diabetes, Endocrinology and Metabolism, School of Medicine, Fukushima Medical University, Fukushima, Japan (M. Shimabukuro).

Accompanying Tables S1, S2 and Figures S1 through S4 are available at https://www.ahajournals.org/doi/suppl/10.1161/JAHA.118.010860

*Dr Fukuda and Dr Nishimoto contributed equally to this work.

Correspondence to: Daiju Fukuda, MD, PhD, Department of Cardio-Diabetes Medicine, Tokushima University Graduate School of Biomedical Sciences, 3-18-15, Kuramoto-cho, Tokushima 770-8503, Japan. E-mail: daiju.fukuda@tokushima-u.ac.jp

Received September 5, 2018; accepted February 25, 2019.

Clinical Perspective

What Is New?

- Angiotensin II infusion to apolipoprotein E-deficient mice (*Apoe*$^{-/-}$) increased circulating levels of cell-free DNA, a ligand for TLR9.
- Genetic deletion or pharmacologic blockade of TLR9 attenuated atherogenesis in angiotensin II–infused *Apoe*$^{-/-}$ mice and the activation of TLR9 promoted proinflammatory activation of macrophages.
- The plasma level of cell-free DNA collected from the target vessel in patients with acute myocardial infarction positively correlated with inflammatory features of target lesions (eg, lipid arc, macrophage content, and ruptured cavity length/area), which were determined by optical coherence tomography.

What Are the Clinical Implications?

- Inhibiting the cell-free DNA–TLR9 axis attenuates proinflammatory activation of macrophages and vascular inflammation and might be a potential therapeutic target for atherosclerotic disease.

the innate immune system by endogenous ligands and subsequent inflammation is involved in various diseases.[6–8] Several studies have shown that inflammation caused by TLR activation by endogenous ligands participates in the development of atherosclerosis.[8–10]

Recent studies have shown the involvement of TLR9 in the pathophysiology of various diseases.[11] TLR9 expressed in endosomes recognizes exogenous DNA fragments that contain unmethylated CpG DNA and plays a role in the innate immune system.[12] In addition, recent evidence has revealed that TLR9 recognizes cell-free DNA (cfDNA) released from degenerated host tissues/cells and stimulates inflammatory cells including macrophages, provoking chronic sterile inflammation. The contribution of cfDNA-TLR9 signaling-associated inflammation is reported in several disease contexts such as autoimmune diseases and others.[13–16] We previously showed that obesity-induced cfDNA released from adipocytes stimulates chronic adipose tissue inflammation and insulin resistance by stimulating macrophages through TLR9.[17]

Atherosclerosis and obesity-induced adipose tissue inflammation share chronic inflammation as an underlying mechanism.[18] Previous studies have shown degeneration of vascular cells including endothelial cells and macrophages in atherosclerotic lesions,[19–22] suggesting the release of cellular debris that contains various endogenous ligands for TLRs. However, the role of cfDNA-TLR9 signaling in atherogenesis remains not fully understood. In this study, we hypothesized that TLR9 activation by cfDNA released in atherosclerotic lesions promotes vascular inflammation and atherogenesis. To address our hypothesis, we induced atherosclerosis in apolipoprotein E–deficient (*Apoe*$^{-/-}$) mice and *Tlr9*-deficient *Apoe*$^{-/-}$ (*Tlr9*$^{-/-}$*Apoe*$^{-/-}$) mice. Here, we infused angiotensin II (Ang II) into both mouse strains to enhance cell death.[23,24] We further investigated the relationship between circulating cfDNA level and coronary plaque characteristics in patients with acute myocardial infarction (MI) to obtain translational evidence for cfDNA-TLR9 signaling in atherogenesis.

Methods

The data that support the findings of this study are available from the corresponding author upon reasonable request.

Animal Experiments

Apoe$^{-/-}$ mice (C57BL/6J background) and *Tlr9*$^{-/-}$ mice (C57BL/6J background) were originally purchased from the Jackson Laboratory and Oriental BioService, Inc, respectively. *Tlr9*$^{-/-}$*Apoe*$^{-/-}$ mice were generated by crossing *Apoe*$^{-/-}$ mice and *Tlr9*$^{-/-}$ mice. Male mice were fed a Western-type diet (WTD; Oriental Yeast Co Ltd) from 6 weeks of age through the completion of the experiment. Ang II, 1000 ng/kg per minute (Wako Pure Chemical Industries, Ltd, Osaka, Japan) was infused by an osmotic pump (Alzet, Cupertino, CA) from 2 weeks after starting a WTD, for 4 weeks. For in vivo TLR9 inhibition, phosphothioate-modified oligodeoxynucleotide—iODN2088 (5′-tcctggcggggaagt-3′) was used. Control (Ctrl)-iODN2088 (5′-tcctgagcttgaagt-3′) was used as its control. These oligodeoxynucleotides were synthesized with a low level of endotoxin (<0.5 endotoxin units/mg; Gene Design Inc., Osaka, Japan) and intraperitoneally injected into Ang II–infused *Apoe*$^{-/-}$ mice (150 μg) three times a week for 4 weeks. All mice were housed under a 12-hour light/dark cycle, with food and water available ad libitum. All experimental procedures conformed to the guidelines for animal experimentation of Tokushima University. The protocol was reviewed and approved by our institutional ethics committee.

Bone Marrow Transplantation

Bone marrow (BM) transplantation was performed as described previously.[17] Six-week-old recipient mice were lethally irradiated (total, 9 Gy). On the following day, unfractionated BM cells harvested from donor mice were injected into recipient mice via tail-vein injection. At 2 weeks after BM transplantation, all mice were started on a WTD, and at 4 weeks after BM transplantation, Ang II infusion was started.

Replacement rate after BM transplantation was determined by fluorescence *in situ* hybridization of the X and Y chromosomes in male recipient mice repopulated with female BM as we described previously.[17] We used only BM chimeric mice, in which >80% of BM had been replaced by donor BM.

Atherosclerotic Lesion Analyses

Atherosclerotic lesions was examined as we reported previously.[25] In brief, mice were euthanized with an overdose of pentobarbital and perfused with 0.9% sodium chloride solution. The heart and aorta were removed immediately. The thoracic aorta was opened longitudinally, and the abdominal aorta was snap-frozen in liquid nitrogen for further analyses. The severity of abdominal aortic aneurysm was determined as reported previously.[26] Atherosclerotic lesions in the aortic arch were determined by en face Sudan IV staining. The characteristics of atherosclerotic plaques were examined in frozen sections of lesions in the aortic root (at 5-μm intervals). Lipid deposition in plaques was determined by oil red O staining. The expression of vascular cell adhesion molecule-1 (VCAM-1) and intercellular cell adhesion molecule-1 (ICAM-1), and accumulation of macrophages in plaques were examined by immunohistochemical staining. Sections were incubated with anti-VCAM-1 antibody (Abcam, Cambridge, MA), anti-ICAM-1 antibody (Abcam), or anti-Mac3 antibody (BD Biosciences, Bedford, MA), followed by the avidin-biotin complex technique and stained using a Vector Red substrate kit (Vector Laboratories, Burlingame, CA). Each section was counterstained with hematoxylin.

Electron Microscopic Analysis

For immunogold staining, samples were fixed in a 4% paraformaldehyde solution containing 0.1% glutaraldehyde and 0.05% Triton X-100 and then embedded in glycol methacrylate. Ultrathin (80–100 nm) sections were incubated with 1% bovine serum albumin in 0.01 mol/L PBS for 1 hour and rinsed with 0.01 mol/L PBS for 15 minutes. The sections were incubated overnight with anti–single-stranded DNA (ssDNA) Rabbit IgG Affinity Purify (Immuno-Biological Laboratories Co Ltd, Gunma, Japan) at 4°C. After the sections were washed with 0.01 mol/L PBS, 10-nm gold-labeled goat anti-rabbit IgG (BBInternational, Cardiff, UK) was applied as the secondary antibody for 2 hours at room temperature. The sections were counterstained with uranyl acetate and Reynold's lead citrate and then examined under an electron microscope (H-7600; Hitachi, Tokyo, Japan). As negative controls for the immunohistochemical procedures, substitution of an identical concentration of nonimmune IgG for the primary antibody and direct incubation in colloidal gold without the primary antibody were performed.

Metabolic Parameter Analyses

At the time of euthanasia, blood was collected into K2-EDTA–containing tubes, and plasma was stored at −80°C until required. Plasma lipid levels were measured at LSI Medience Corporation (Tokyo, Japan). Blood pressure was measured using a tail-cuff system (BP-98A, Softron, Tokyo, Japan). The averaged value of three measurements in conscious mice was used for comparison.

Measurement of Plasma cfDNA Level

cfDNA in plasma was extracted using a QIAamp DNA Mini Kit (Qiagen, Venlo, the Netherlands). The concentrations of double-stranded DNA (dsDNA) and ssDNA in extracted cfDNA were measured using a Quant-iT PicoGreen dsDNA Assay Kit (Life Technologies, Carlsbad, CA) and QuantiFluor ssDNA System (Promega, Madison, WI), respectively.

Cell Culture Experiments

Thioglycolate-induced peritoneal macrophages were collected from female *Apoe*$^{-/-}$ mice and *Tlr9*$^{-/-}$*Apoe*$^{-/-}$ mice at 8 to 10 weeks of age and cultured in Dulbecco's modified Eagle's medium containing 10% fetal bovine serum. Isolated peritoneal macrophages were used for experiments 24 hours after seeding. Peritoneal macrophages were stimulated with CpG-ODN1826 (ODN1826), a specific oligonucleotide that activates TLR9, or its control (Ctrl-ODN1826) (Gene Design Inc., Osaka, Japan) for 4 hours to examine gene expression or for 45 minutes to examine p38 mitogen-activated protein kinase (MAPK) phosphorylation. To inhibit TLR9 or p38 MAPK, cells were treated with iODN2088 or SB203580 (Abcam, Cambridge, MA), respectively. Treated cells were used for gene expression or protein expression analyses.

Genomic DNA (gDNA) of macrophages was extracted using a QIAamp DNA Mini Kit (Qiagen, Venlo, the Netherlands), and transfected into *Apoe*$^{-/-}$ macrophages or *Tlr9*$^{-/-}$*Apoe*$^{-/-}$ macrophages using Lipofectamine® LTX with Plus™ Reagent (Thermo Fisher Scientific, Waltham, MA) according to the manufacturer's instructions.

Real-Time Reverse-Transcription Polymerase Chain Reaction

cDNA was synthesized using a QuantiTect Reverse Transcription kit (Qiagen, Venlo, the Netherlands) from total RNA extracted from tissues or cells using an illustra RNAspin RNA Isolation Kit (GE Healthcare, Chicago, IL). Quantitative real-time polymerase chain reaction (qPCR) was performed on Mx3000P (Agilent Technologies, Santa Clara, CA) using gene-specific primers (Table S1) and Power SYBR Green PCR

Master Mix (Applied Biosystems, Foster City, CA). Data are expressed in arbitrary units normalized by β-actin.

Western Blotting Analysis

Lysates prepared from cells or aorta in RIPA buffer (Wako Pure Chemical Industries, Ltd, Osaka, Japan) containing a protease inhibitor cocktail (Roche, Basel, Switzerland) and a phosphatase inhibitor cocktail (Thermo Fisher Scientific) were separated on SDS–polyacrylamide gel electrophoresis gels. The following antibodies were used: anti-TLR9, anti-VCAM-1 (Abcam, Cambridge, MA), anti-p38 MAPK, anti-phospho-p38 MAPK (Cell Signaling, Danvers, MA), and anti-β-actin (Sigma, Fukushima, Japan). Levels of expression were quantified by densitometry (ImageQuant LAS 4000mini; GE Healthcare Life Sciences, Little Chalfont, England).

Enzyme Linked Immunosolvent Assay

To detect proinflammatory activation of macrophages, we performed ELISA using culture supernatant of macrophages: *Apoe*$^{-/-}$ macrophages or *Tlr9*$^{-/-}$*Apoe*$^{-/-}$ macrophages were cultured with ODN1826 or Ctrl-ODN1826 for 24 hours, and then culture supernatant was collected after centrifugation and filtration through a 20-μm mesh to remove cell debris. Levels of monocyte chemoattractant protein-1 (MCP-1) and tumor necrosis factor-α (TNF-α) in culture supernatant were measured using commercially available kit (Proteintech, Chicago, IL).

Clinical Research

We included patients with acute MI including both ST-segment elevation MI or non–ST-segment elevation MI who underwent emergency percutaneous coronary intervention and optical coherence tomography (OCT) study of the vessel undergoing percutaneous coronary intervention at Wakayama Medical University Hospital. The diagnostic criteria for these disease conditions were described in the previous study.[27] Patients with hemodynamic shock, renal insufficiency with baseline creatinine >1.6 mg/dL (or estimated glomerular filtration rate <35 mL/min per 1.73 m^2), known systemic inflammatory conditions requiring corticosteroid therapy, evidence of active infectious diseases, a left main coronary artery lesion, an extremely tortuous vessel, or reference vessel diameter >4 mm were excluded. In addition, we excluded patients with poor OCT images. This protocol was approved by the Wakayama Medical University Ethics Committee. All patients provided written informed consent before participation. This study was in compliance with the Declaration of Helsinki with regard to investigations on humans.

Primary percutaneous coronary intervention was performed in all patients. Coronary angiography was performed using a 5-Fr Judkins-type catheter via the femoral or radial approach. All patients received oral aspirin, an intravenous bolus injection of 5000 U heparin, and intracoronary isosorbide dinitrate before angiography. After completion of diagnostic angiography, the culprit lesion was identified on the basis of coronary angiography findings as well as those of electrocardiography and echocardiography. Before manual thromboaspiration, blood was collected from coronary arteries using an aspiration catheter (Export; Medtronic Japan, Tokyo, Japan). All samples were immediately centrifuged at 3000*g* for 15 minutes, and then stored at −80°C. Following thromboaspiration, frequency domain OCT (ILUMIEN and ILUMIEN OPTIS, St. Jude Medical, Minnesota, USA; or LUNAWAVE, Terumo, Tokyo, Japan) was used to observe the culprit lesion morphology. No patients were administered glycoprotein IIa/IIIb inhibitors because their use is not approved in Japan.

All OCT images were analyzed using commercially available offline OCT consoles as described previously.[27] For OCT image analysis, consensus reading was performed by 2 experienced OCT investigators (A.T. and T.N.) who were blinded to the angiographic and clinical data. Macrophages were assessed using a previously reported technique.[28] In short, macrophage accumulation was defined as high-intensity, signal-rich linear regions with sharp attenuation. Maximum lipid arc was also measured.[29] The cross-sectional area of the ruptured cavity at the site of the largest intraplaque cavity and longitudinal cavity length were measured according to the previous study.[30] Four patients were excluded from the analysis of cavity area/length because clear cavity images were not obtained because of thrombi.

Statistical Analyses

All numerical values are expressed as mean±SEM. Comparison of parameters between 2 groups was performed with unpaired Student *t* test when data showed a normal distribution or with Mann–Whitney *U* test when data did not show a normal distribution. The utilized nonparametric test (Mann–Whitney) is based on ranks and thus less sensitive to the magnitude of outliers. The severity of abdominal aortic aneurysm and survival curve between the 2 strains were analyzed by Mann–Whitney *U* test and Kaplan–Meier method with log-rank test, respectively. Univariate analysis between plaque characteristics and plasma dsDNA or ssDNA level was performed using Spearman's rank correlation coefficient. A value of $P<0.05$ was considered significant.

Results

Angiotensin II Increases Circulating cfDNA in Plasma and TLR9 Expression in Atherosclerotic Aorta

To stimulate cell death and atherogenesis, we administered Ang II to animals. Ang II infusion for 4 weeks significantly elevated circulating level of dsDNA in both *Apoe*$^{-/-}$ mice and *Tlr9*$^{-/-}$*Apoe*$^{-/-}$ mice, and ssDNA in *Tlr9*$^{-/-}$*Apoe*$^{-/-}$ mice (Figure 1A and 1B). Ang II infusion also increased the expression of TLR9, a receptor for cfDNA, at the RNA and protein level in the atherosclerotic aorta in *Apoe*$^{-/-}$ mice (Figure 1C and 1D). Immunoelectron microscopic analysis using atherosclerotic plaques demonstrated accumulation of ssDNA in the cytoplasm of macrophages, suggesting that macrophages take up cfDNA in atherosclerotic lesions (Figure 1E).

Genetic Deletion of TLR9 in *Apoe*$^{-/-}$ Mice Attenuates Vascular Inflammation and Atherogenesis

We compared atherosclerotic lesion progression in the aortic arch between *Apoe*$^{-/-}$ mice and *Tlr9*$^{-/-}$*Apoe*$^{-/-}$ mice after 4 weeks of Ang II infusion. Blood pressure and levels of lipids such as total cholesterol, high-density lipoprotein cholesterol, and triglyceride were comparable between the two mouse strains (Table 1). The results of en face Sudan IV staining demonstrated a significant reduction in atherosclerotic lesions in *Tlr9*$^{-/-}$*Apoe*$^{-/-}$ mice compared with *Apoe*$^{-/-}$ mice (Figure 2A). The results of qPCR analysis indicated that genetic deletion of TLR9 reduced the expression of inflammatory molecules such as VCAM-1 ($P<0.05$), ICAM-1 ($P<0.01$), and MCP-1 ($P<0.05$) in the aorta. Deletion of *Tlr9* tended to decrease the expression of TNF-α and F4/80, a macrophage marker, in the aorta (Figure 2B). Oil red O staining of atherosclerotic plaques in the aortic root demonstrated that *Tlr9* deficiency decreased lipid deposition in plaques in *Apoe*$^{-/-}$ mice ($P<0.01$) (Figure 3A). Immunohistochemical analysis showed that the expression of VCAM-1 ($P<0.001$) and ICAM-1 ($P<0.05$) was lower in *Tlr9*$^{-/-}$*Apoe*$^{-/-}$ mice than in *Apoe*$^{-/-}$ mice (Figure 3B and 3C). Also, infiltration of macrophages into atherosclerotic plaques determined by Mac3 staining was reduced in *Tlr9*$^{-/-}$*Apoe*$^{-/-}$ mice compared with *Apoe*$^{-/-}$ mice ($P<0.05$) (Figure 3D). These results suggested reduced vascular inflammation in *Tlr9*$^{-/-}$*Apoe*$^{-/-}$ mice compared with *Apoe*$^{-/-}$ mice. There was no significant difference in the severity of aortic aneurysm and survival between 2 strains of mice in this study (Figure S1).

Administration of TLR9 Antagonist Attenuates Vascular Inflammation and Atherogenesis in *Apoe*$^{-/-}$ Mice

To confirm the role of TLR9 in the development of vascular inflammation and atherosclerosis in Ang II–infused *Apoe*$^{-/-}$ mice, we examined whether pharmacologic inhibition of TLR9 attenuates vascular inflammation and atherogenesis. Administration of an inhibitory oligonucleotide of TLR9, iODN2088, significantly suppressed atherosclerotic lesion development in *Apoe*$^{-/-}$ mice compared with its control as determined by en face Sudan IV staining in the aortic arch ($P<0.05$) (Figure 4A). iODN2088 did not alter metabolic parameters including blood pressure and plasma lipid levels (Table 2). The results of qPCR analysis showed that iODN2088 treatment decreased the expression of inflammatory molecules, such as ICAM-1 and MCP-1, and a macrophage marker in the atherosclerotic aorta (Figure 4B). Histologic analyses demonstrated that inhibition of TLR9 reduced the expression of VCAM-1 ($P<0.01$) and macrophage accumulation ($P<0.001$) in atherosclerotic plaques in *Apoe*$^{-/-}$ mice. iODN2088 treatment decreased lipid deposition and ICAM-1 expression, although these did not reach statistical significance (Figure 5A through 5D). These results suggested that in vivo TLR9 blockade partially attenuates the development of vascular inflammation and atherosclerosis.

Restoration of TLR9 in BM Stimulates Atherogenesis in *Tlr9*$^{-/-}$*Apoe*$^{-/-}$ Mice

Immune cells such as macrophages are the major population which expresses TLR9. Therefore, to examine the role of TLR9 in atherogenesis, we restored TLR9 in BM in *Tlr9*$^{-/-}$*Apoe*$^{-/-}$ mice. Atherosclerotic lesion development under Ang II infusion was significantly greater in mice that express TLR9 in BM than mice that lack TLR9 in BM ($P<0.05$) (Figure 6A). We also examined the expression of inflammatory molecules in the aorta. The expression of a macrophage marker was significantly higher in the mice that have TLR9 in BM compared with the mice that lack TLR9 in BM ($P<0.05$). The expression of other inflammatory molecules showed the same tendency; however, it did not reach statistical significance (Figure 6B). There were no differences in metabolic parameters between these mice (Table 3).

TLR9 Signaling Promotes Macrophage Activation

We investigated the role of TLR9 in macrophage activation, an essential feature of vascular inflammation and atherogenesis. TLR9 activation by ODN1826, a TLR9 agonist, promoted the expression of inflammatory molecules such as VCAM-1 and ICAM-1 in *Apoe*$^{-/-}$ macrophages, but not in *Tlr9*$^{-/-}$*Apoe*$^{-/-}$

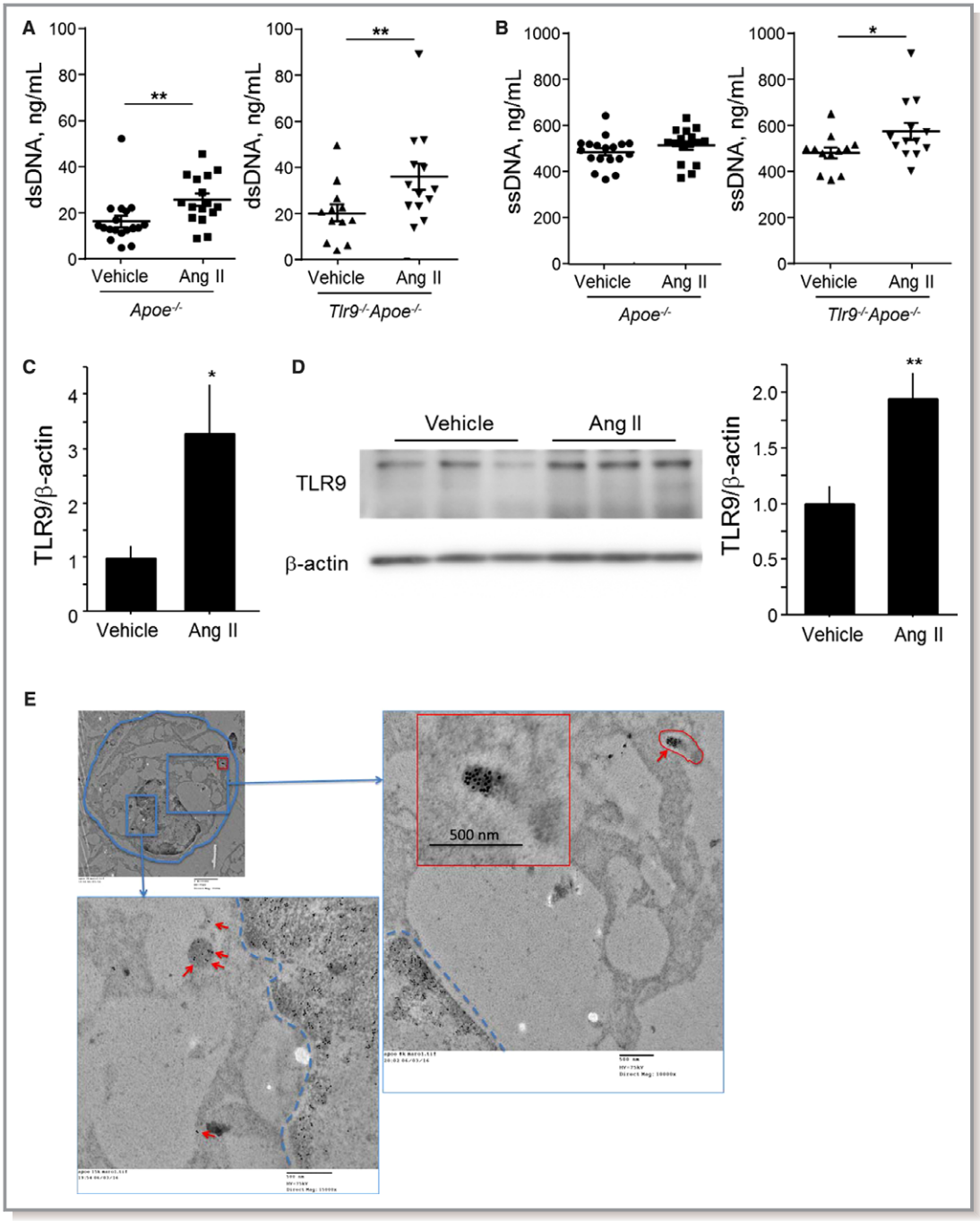

Figure 1. Angiotensin II increases circulating cfDNA and TLR9 expression in atherosclerotic aorta. **A** and **B**, Ang II infusion for 4 weeks to WTD-fed *Apoe*$^{-/-}$ mice and *Tlr9*$^{-/-}$*Apoe*$^{-/-}$ mice increased circulating cfDNA as determined by dsDNA and ssDNA (n=12–18). Comparison between Ang II-treated group and vehicle-treated group in each strain was performed with Mann–Whitney *U* test. **C** and **D**, Ang II infusion for 4 weeks to WTD-fed *Apoe*$^{-/-}$ mice promoted TLR9 expression at the RNA (**C**) and protein (**D**) level in the atherosclerotic aorta. Comparison between Ang II–treated group and vehicle-treated group was performed with Mann–Whitney *U* test. **E**, Representative immunogold staining against ssDNA demonstrated the accumulation of gold particles (10 nm) in the cytoplasm of macrophages (arrows) in atherosclerotic lesions obtained from WTD-fed *Apoe*$^{-/-}$ mice. Scale bar, 500 nm. Inset: lower magnification (scale bar, 2 μm). **P*<0.05 and ***P*<0.01. All values are mean±SEM. Ang II indicates angiotensin II; cfDNA, cell-free DNA; dsDNA, double-stranded DNA; ssDNA, single-stranded DNA; TLR9, Toll-like receptor 9; WTD, Western-type diet.

Table 1. Effect of Genetic Deletion of TLR9 on Metabolic Parameters

	Apoe$^{-/-}$	*Tlr9*$^{-/-}$*Apoe*$^{-/-}$	*P* Value
Body weight, g	29.9±1.0	29.5±0.7	0.72
Heart rate, bpm	713±10	701±15	0.58
Systolic blood pressure, mm Hg	134.6±4.3	126.4±2.8	0.19
Diastolic blood pressure, mm Hg	88.2±2.9	83.4±2.9	0.25
Total cholesterol, mg/dL	1361.7±75.8	1251.8±105.3	0.51
Triglyceride, mg/dL	168.9±15.8	190.7±24.3	0.46
HDL cholesterol, mg/dL	20.6±2.3	20.0±1.6	0.85

All values are mean±SEM. HDL indicates high-density lipoprotein; TLR9, Toll-like receptor 9.

macrophages (Figure 7A). iODN2088, a specific antagonist of TLR9, completely inhibited these responses (Figure S2). Proinflammatory activation of macrophages was also confirmed at the protein level (Figure 7B and 7C).

TLR9 is a receptor for DNA fragments released from degenerated cells. Therefore, we prepared gDNA from macrophages and transfected it into *Apoe*$^{-/-}$ or *Tlr9*$^{-/-}$*Apoe*$^{-/-}$ macrophages. gDNA promoted inflammatory molecule (eg, VCAM-1, ICAM-1, and

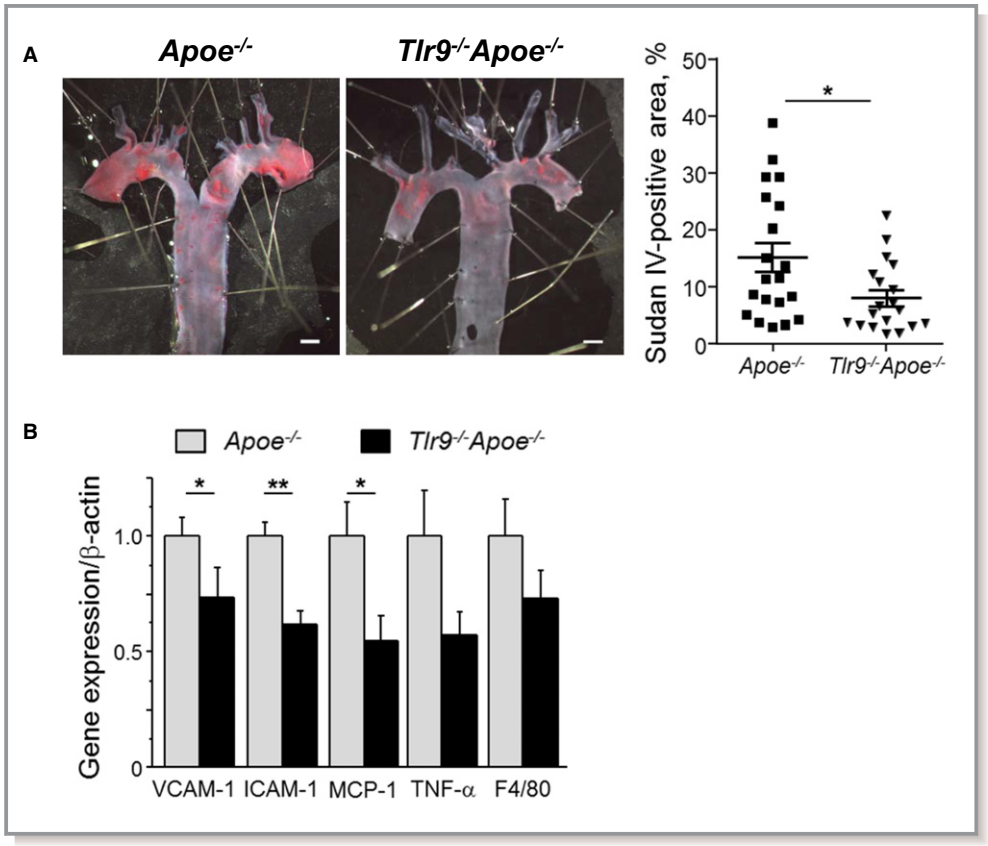

Figure 2. Genetic deletion of TLR9 in *Apoe*$^{-/-}$ mice attenuates atherogenesis and vascular inflammation. **A**, En face Sudan IV staining of the aortic arch showed that *Tlr9*$^{-/-}$*Apoe*$^{-/-}$ mice had reduced atherosclerotic lesions compared with *Apoe*$^{-/-}$ mice (n=19–20). Bar: 1 mm. **B**, qPCR analysis using the abdominal aorta revealed that genetic deletion of TLR9 decreased the expression of inflammatory molecules such as VCAM-1, ICAM-1, and MCP-1. TLR9 deletion tended to reduce the expression of TNF-α and F4/80, a macrophage marker, in the atherosclerotic aorta (n=13–14). **P*<0.05 and ***P*<0.01. All comparisons between *Tlr9*$^{-/-}$*Apoe*$^{-/-}$ mice and *Apoe*$^{-/-}$ mice were performed with Mann–Whitney *U* test. All values are mean±SEM. ICAM-1 indicates intercellular cell adhesion molecule-1; MCP-1, monocyte chemoattractant protein-1; qPCR, quantitative real-time polymerase chain reaction; TLR9, Toll-like receptor 9; TNF- α, tumor necrosis factor-α; VCAM-1, vascular cell adhesion molecule-1.

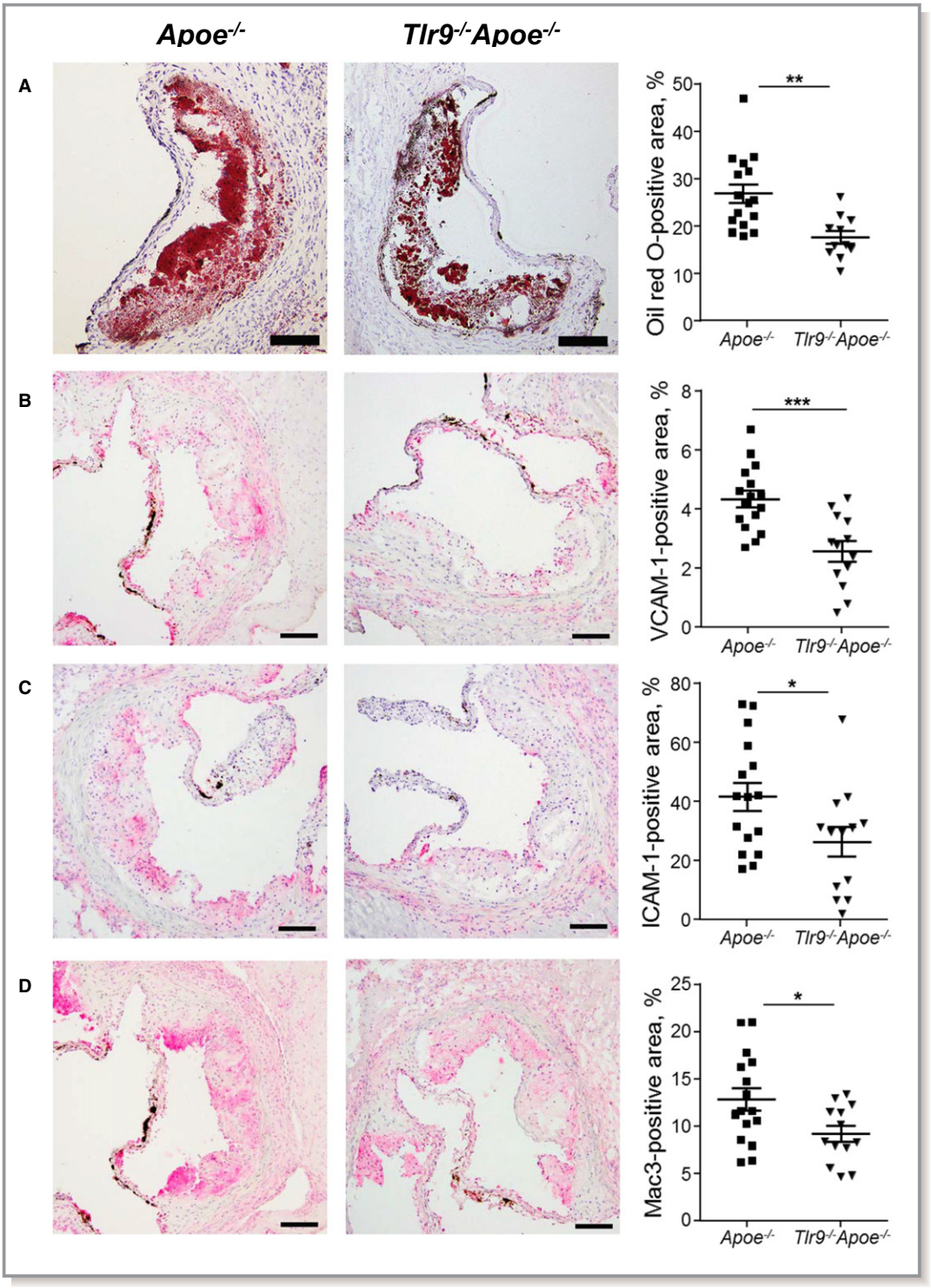

Figure 3. Genetic deletion of TLR9 in *Apoe*$^{-/-}$ mice reduces inflammatory molecule expression in atherosclerotic plaques. **A**, Oil red O staining of atherosclerotic plaques in the aortic root. Lipid deposition in plaques was decreased in *Tlr9*$^{-/-}$*Apoe*$^{-/-}$ mice compared with that in *Apoe*$^{-/-}$ mice (n=11–16). Bar: 100 μm. **B** through **D**, Immunostaining against VCAM-1 (**B**), ICAM-1 (**C**), and Mac3 (**D**). Genetic deletion of TLR9 reduced the expression of adhesion molecules and accumulation of macrophages in atherosclerotic plaques in *Apoe*$^{-/-}$ mice (n=13–16). Bar: 100 μm. **P*<0.05, ***P*<0.01, and ****P*<0.001. All comparisons between *Tlr9*$^{-/-}$*Apoe*$^{-/-}$ mice and *Apoe*$^{-/-}$ mice were performed with unpaired Student *t* test. All values are mean±SEM. ICAM-1 indicates intercellular cell adhesion molecule-1; TLR9, Toll-like receptor 9; VCAM-1, vascular cell adhesion molecule-1.

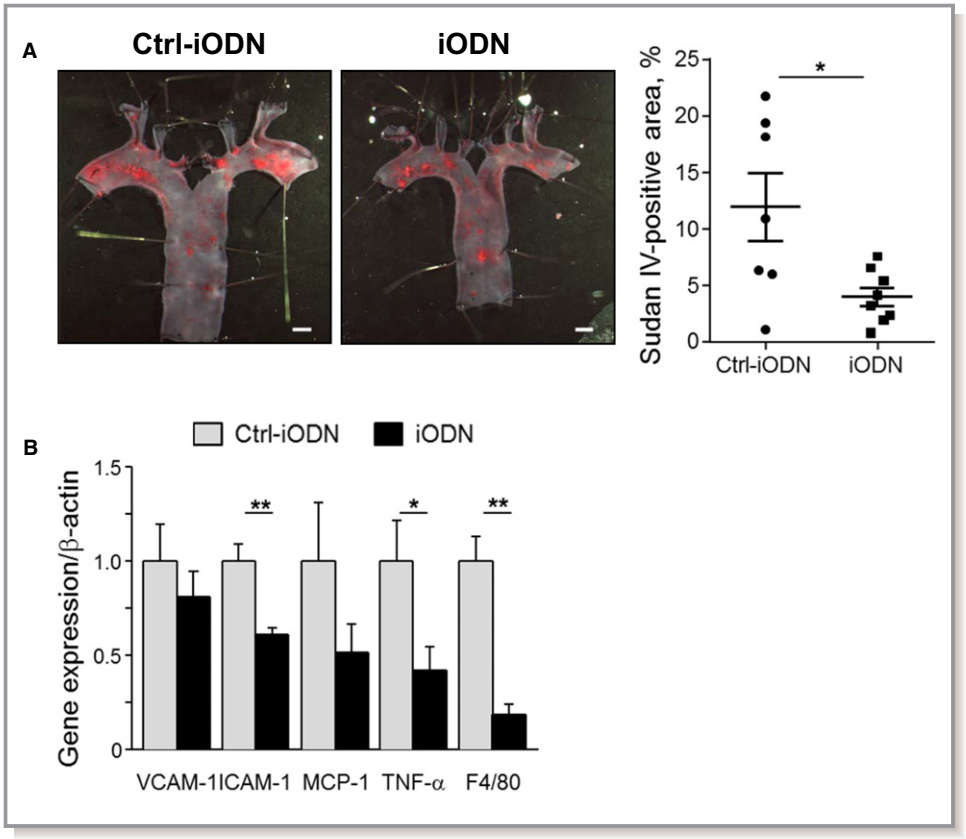

Figure 4. Administration of TLR9 antagonist attenuates atherogenesis and vascular inflammation in *Apoe*$^{-/-}$ mice. **A**, En face Sudan IV staining of the aortic arch showed that administration of iODN2088, an inhibitory oligonucleotide for TLR9, to Ang II–infused *Apoe*$^{-/-}$ mice reduced atherosclerotic lesion development compared with control oligonucleotide administration, Ctrl-iODN (n=7–8). Bar: 1 mm. **B**, qPCR analysis using abdominal aorta revealed that iODN2088 treatment decreased the expression of inflammatory molecules such as VCAM-1, ICAM-1, and MCP-1. TLR9 deletion also reduced the expression of F4/80, a macrophage marker, and TNF-α in the atherosclerotic aorta (n=7–8). **P*<0.05 and ***P*<0.01. All comparisons between iODN2088-treated group and Ctrl-iODN–treated group were performed with Mann–Whitney *U* test. All values are mean±SEM. ICAM-1 indicates intercellular cell adhesion molecule-1; MCP-1, monocyte chemoattractant protein-1; qPCR, quantitative real-time polymerase chain reaction; TLR9, Toll-like receptor 9; TNF- α, tumor necrosis factor-α; VCAM-1, vascular cell adhesion molecule-1.

MCP-1) expression more effectively in *Apoe*$^{-/-}$ macrophages than in *Tlr9*$^{-/-}$*Apoe*$^{-/-}$ macrophages (Figure 7D).

The results of Western blotting analysis showed that ODN1826 increased the phosphorylation of p38 MAPK in *Apoe*$^{-/-}$ macrophages (Figure 8A and Figure S3). Furthermore, a p38 MAPK inhibitor, SB203580, attenuated ODN1826-induced expression of inflammatory molecules (Figure 8B). These results indicated that activation of MAPK signaling participates in the TLR9-mediated inflammatory response of macrophages at least partially.

Circulating cfDNA Is Associated With Plaque Vulnerability in Humans

To investigate the clinical significance of cfDNA, we examined the relationship between plaque characteristics determined by OCT and circulating cfDNA in the coronary artery in patients with acute MI. The patients' background is summarized in Table 4. Mean age of the participants was 70.0±1.8 years; 64% were male. dsDNA level positively correlated with lipid arc (Spearman ρ=0.32; *P*<0.05) and macrophage grade (Spearman ρ=0.32; *P*<0.05). dsDNA level also correlated with cavity length (Spearman ρ=0.46; *P*<0.01) and tended to correlate with cavity area (Spearman ρ=0.31; *P*=0.07) in coronary artery plaques (Figure 9A through 9D). ssDNA level significantly correlated with lipid arc (Spearman ρ=0.36; *P*<0.05) and cavity length (Spearman ρ=0.36; *P*<0.05), and tended to correlate with macrophage grade and cavity area (Figure 9E through 9H). These results indicated that cfDNA level is associated with the features of vulnerable atherosclerotic plaques, implying participation of cfDNA-TLR9 signaling in the development of vascular inflammation in coronary arteries in humans.

Table 2. Effect of Pharmacologic Blockade of TLR9 on Metabolic Parameters

	Ctrl-iODN2088	iODN2088	*P* Value
Body weight, g	33.9±0.9	32.3±1.1	0.31
Heart rate, bpm	696±12	721±15	0.21
Systolic blood pressure, mm Hg	143.4±8.1	139.5±6.6	0.70
Diastolic blood pressure, mm Hg	88.9±2.3	91.4±4.5	0.64
Total cholesterol, mg/dL	1250.7±84.5	1060.6±173.6	0.36
Triglyceride, mg/dL	135.4±21.7	161.4±32.7	0.53
HDL cholesterol, mg/dL	20.1±1.1	18.3±3.5	0.64

All values are mean±SEM. HDL indicates high-density lipoprotein; TLR9, Toll-like receptor 9.

Discussion

Accumulating evidence suggests that atherosclerosis is a chronic inflammatory disease[1]; however, the mechanism of vascular inflammation and atherogenesis is not fully understood. In this study, we demonstrated that Ang II treatment increased the level of plasma cfDNA, an endogenous ligand for TLR9. Also, genetic deletion of TLR9 or pharmacologic blockade of TLR9 revealed that TLR9 plays a pivotal role in the development of vascular inflammation and atherogenesis in Ang II–infused *Apoe*$^{-/-}$ mice. On the other hand, restoration of TLR9 in BM promoted atherogenesis in TLR9-deficient mice. Results of in vitro experiments showed that TLR9 activation promotes proinflammatory activation of macrophages via p38 MAPK at least partially, supporting the results of our in vivo studies. Furthermore, in our clinical study, circulating cfDNA level in the coronary artery was associated with vulnerable features of atherosclerotic plaques in the coronary artery. These results suggested the participation of cfDNA-TLR9 signaling in the development of vascular inflammation and atherosclerosis.

TLR activation by endogenous ligands released as damage-associated molecular patterns in response to various risk factors has attracted much attention as a possible mechanism of vascular inflammation and atherosclerosis.[9,15] For example, previous studies have reported that activation of TLR2 or TLR4 by their endogenous ligands, such as fatty acids, lipoproteins, and heat shock proteins, promotes atherogenesis.[31–33] Recent studies including our own have suggested that TLR9 recognizes cfDNA as an endogenous ligand, promoting chronic inflammation.[11,16,17] However, the role of TLR9 in atherogenesis is still controversial.

In the present study, we found that Ang II infusion into *Apoe*$^{-/-}$ mice increased the expression of *Tlr9* in the aorta. Also, immunoelectron microscopic analysis demonstrated the accumulation of ssDNA in macrophages in atherosclerotic lesions. Therefore, to test the hypothesis that the cfDNA-TLR9 pathway plays a pivotal role in the progression of vascular inflammation in vivo, we employed 3 mouse models. In addition, we infused Ang II into animals to enhance vascular damage, which accelerates release of cfDNA.[23,24] In fact, Ang II infusion increased plasma cfDNA in both mouse strains. Genetic deletion of TLR9 attenuated the development of vascular inflammation and atherogenesis in *Apoe*$^{-/-}$ mice under Ang II infusion. Pharmacologic blockade of TLR9 using a specific TLR9 antagonist also suppressed vascular inflammation and atherogenesis in Ang II–infused *Apoe*$^{-/-}$ mice. On the other hand, restoration of TLR9 in BM promoted atherogenesis partially in TLR9-deficient animals under Ang II infusion. These results demonstrated that TLR9 stimulates atherosclerosis in *Apoe*$^{-/-}$ mice, at least partially, under an Ang II–infused condition. To investigate the mechanism, we examined the role of TLR9 in proinflammatory activation of macrophages, a key player in atherogenesis.[34,35] Ligation of a TLR9 agonist to macrophages promoted expression of inflammatory molecules such as TNF-α, ICAM-1, and VCAM-1. TLR9-deficient macrophages did not show this response. The increase of adhesion molecules in *Apoe*$^{-/-}$ macrophages may explain the increase of macrophage infiltration into plaques. We further transfected gDNA extracted from macrophages into *Apoe*$^{-/-}$ and *Tlr9*$^{-/-}$*Apoe*$^{-/-}$ macrophages. Previous studies have shown the degradation of vascular cells such as endothelial cells or smooth muscle cells in atherosclerotic lesions,[19] whereas recent studies also demonstrated degradation of macrophages in lesions, which is associated with the progression or vulnerability of atherosclerotic plaques.[22] gDNA more strongly promoted inflammatory molecule expression in *Apoe*$^{-/-}$ macrophages than in *Tlr9*$^{-/-}$*Apoe*$^{-/-}$ macrophages. We also found that TLR9 activation increased the phosphorylation of p38 MAPK signaling, an important pathway for inflammatory activation,[36,37] in *Apoe*$^{-/-}$ macrophages. This result is consistent with previous studies demonstrating a link between TLR9 and MAPK.[38] In fact, a p38 MAPK inhibitor attenuated the expression of inflammatory molecules induced by a TLR9 agonist in *Apoe*$^{-/-}$ macrophages. These results suggested

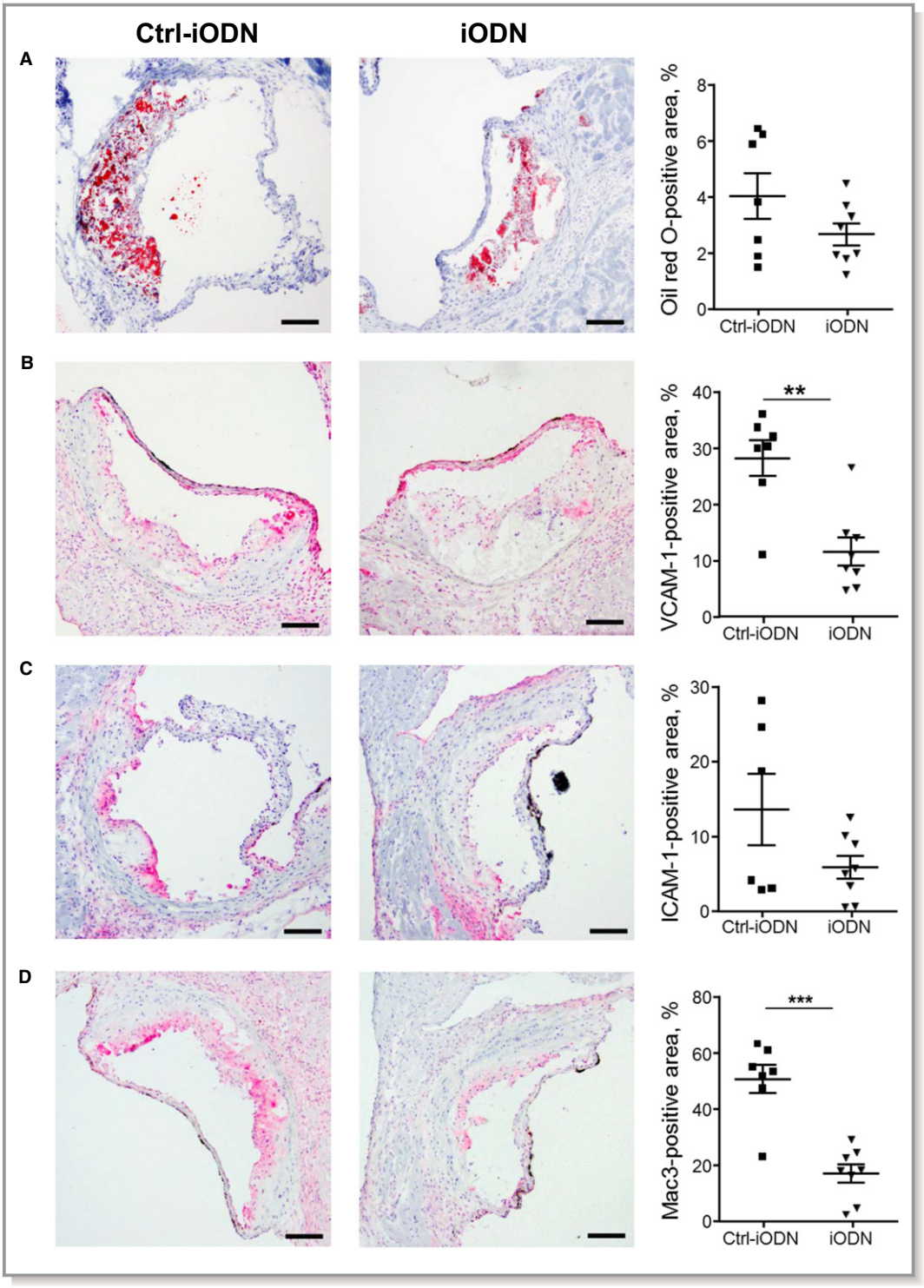

Figure 5. Administration of TLR9 antagonist reduces inflammatory molecule expression in atherosclerotic plaques. **A**, Oil red O staining of atherosclerotic plaques in the aortic root. iODN2088 reduced lipid deposition in atherosclerotic plaques compared with Ctrl-iODN; however, this did not reach statistical significance (n=7–8). Bar: 100 μm. **B** through **D**, Immunostaining against VCAM-1 (**B**), ICAM-1 (**C**), and Mac3 (**D**). iODN2088 reduced the expression of VCAM-1 and the accumulation of macrophages in atherosclerotic plaques compared with Ctrl-iODN (n=7–8). Bar: 100 μm. $^{**}P<0.01$ and $^{***}P<0.001$. All comparisons between iODN2088-treated group and Ctrl-iODN–treated group were performed with unpaired Student *t* test. All values are mean±SEM. ICAM-1 indicates intercellular cell adhesion molecule-1; TLR9, Toll-like receptor 9; TNF- α, tumor necrosis factor-α; VCAM-1, vascular cell adhesion molecule-1.

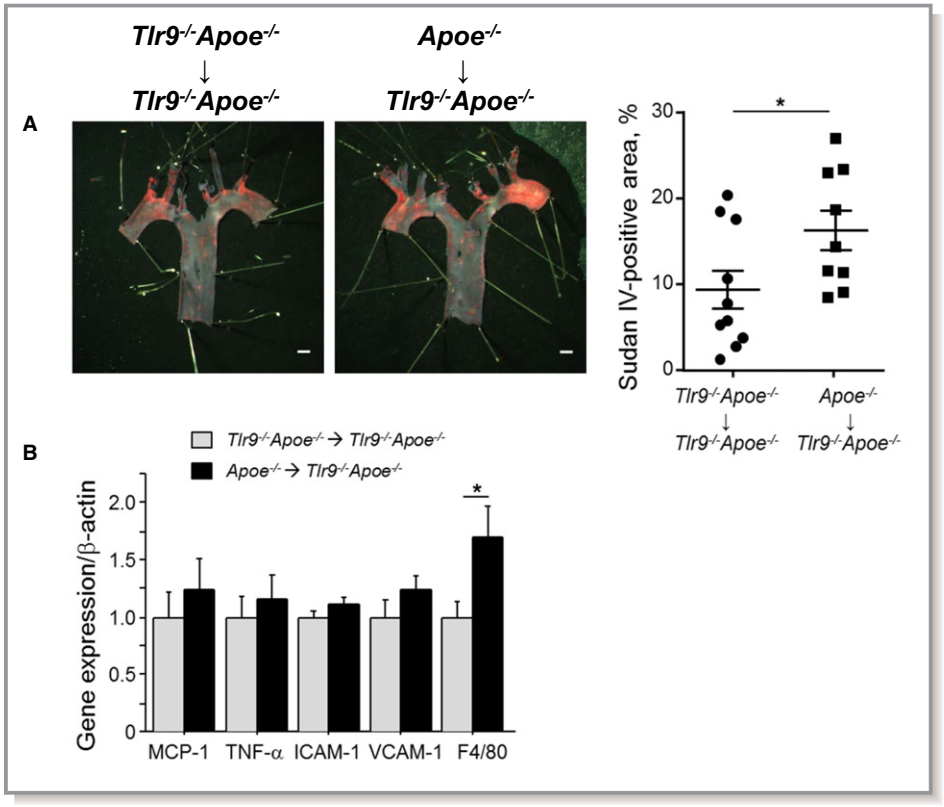

Figure 6. Restoration of TLR9 in BM promotes atherogenesis in *Tlr9*$^{-/-}$*Apoe*$^{-/-}$ mice. **A**, En face Sudan IV staining of the aortic arch showed that restoration of TLR9 in BM promoted atherogenesis in *Tlr9*$^{-/-}$*Apoe*$^{-/-}$ mice under Ang II infusion (n=9–10). Bar: 1 mm. **B**, qPCR analysis using abdominal aorta revealed that restoration of TLR9 in BM promoted the expression of a macrophage marker, F4/80 (n=9–10). **P*<0.05. All comparisons between two BM-chimeric mice were performed with Mann–Whitney *U* test. All values are mean±SEM. BM indicates bone marrow; ICAM-1, intercellular cell adhesion molecule-1; MCP-1, monocyte chemoattractant protein-1; qPCR, quantitative real-time polymerase chain reaction; TLR9, Toll-like receptor 9.

that cfDNA-TLR9 signaling stimulates proinflammatory activation of macrophages and the development of atherosclerosis. Some previous studies have demonstrated that pharmacologic inactivation or activation of TLR9 in *Apoe*$^{-/-}$ mice suppressed or promoted atherosclerotic lesion development, respectively, indicating a proatherogenic role of

Table 3. Effect of Restoration of TLR9 in Bone Marrow on Metabolic Parameters

Donor	*Tlr9*$^{-/-}$*Apoe*$^{-/-}$	*Apoe*$^{-/-}$	
↓	↓	↓	
Recipient	*Tlr9*$^{-/-}$*Apoe*$^{-/-}$	*Tlr9*$^{-/-}$*Apoe*$^{-/-}$	*P* Value
Body weight, g	26.6±0.8	25.6±1.0	0.45
Heart rate, bpm	656±31	680±31	0.59
Systolic blood pressure, mm Hg	138.9±4.3	136.9±4.3	0.75
Diastolic blood pressure, mm Hg	93.6±4.4	87.6±4.9	0.38
Total cholesterol, mg/dL	1407.6±295.8	1884.5±81.1	0.11
Triglyceride, mg/dL	145.1±34.8	168.6±20.3	0.57
HDL cholesterol, mg/dL	20.4±3.8	19.0±1.4	0.74

All values are mean±SEM. HDL indicates high-density lipoprotein; TLR9, Toll-like receptor 9.

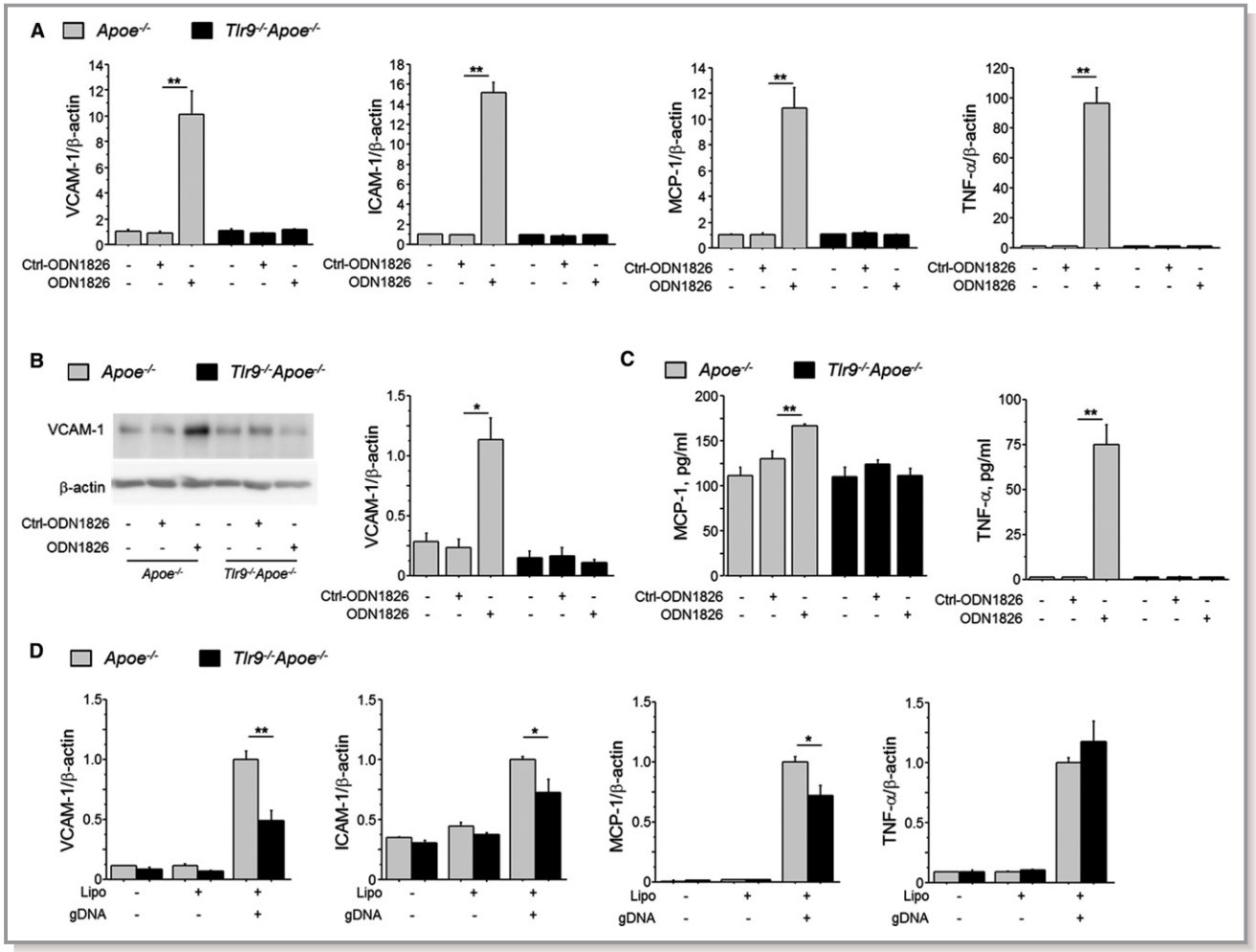

Figure 7. TLR9 signaling promotes macrophage activation. **A**, ODN1826 (100 nmol/L), a TLR9-specific ligand, increased the expression of inflammatory molecules, such as VCAM-1, ICAM-1, MCP-1, and TNF-α in peritoneal macrophages obtained from *Apoe*$^{-/-}$ mice, but not in macrophages obtained from *Tlr9*$^{-/-}$*Apoe*$^{-/-}$ mice (n=6). **B**, Western blotting demonstrated that TLR9 activation with ODN1826 (100 nmol/L) increased the expression of VCAM-1 in *Apoe*$^{-/-}$ macrophages, but not in *Tlr9*$^{-/-}$*Apoe*$^{-/-}$ macrophages (n=5). **C**, ELISA demonstrated that TLR9 activation with ODN1826 (100 nmol/L) increased TNF-α and MCP-1 in supernatant of *Apoe*$^{-/-}$ macrophages, but not in that of *Tlr9*$^{-/-}$*Apoe*$^{-/-}$ macrophages (n=5). **D**, Transfection of gDNA promoted the expression of VCAM-1, ICAM-1, and MCP-1 in *Apoe*$^{-/-}$ macrophages, but not in *Tlr9*$^{-/-}$*Apoe*$^{-/-}$ macrophages (n=5–6). **P*<0.05 and ***P*<0.01. **A** through **C**, Comparisons between ODN1826-treated group and Ctrl-ODN1826-treated group in each mouse strain were performed with Mann–Whitney *U* test. **D**, Comparisons between *Tlr9*$^{-/-}$*Apoe*$^{-/-}$ macrophages and *Apoe*$^{-/-}$ macrophages were performed with Mann–Whitney *U* test. All values are mean±SEM. gDNA indicates genomic DNA; ICAM-1, intercellular cell adhesion molecule-1; MCP-1, monocyte chemoattractant protein-1; qPCR, quantitative real-time polymerase chain reaction; TLR9, Toll-like receptor 9; TNF- α, tumor necrosis factor-α; VCAM-1, vascular cell adhesion molecule-1.

TLR9.[39,40] The results of our present study are consistent with previous studies and provide the mechanism for TLR9 activation in atherosclerosis partially.

On the other hand, a recent study by Koulis et al demonstrated antiatherogenic roles of TLR9 by using a genetic deletion model of TLR9 in *Apoe*$^{-/-}$ mice.[41] In that study, not only genetic deletion but also administration of ODN1668, another TLR9 agonist, inhibited atherosclerotic lesion development in *Apoe*$^{-/-}$ mice on a WTD. In that study, atherosclerosis was induced by long-term WTD feeding but not Ang II. While, in our present study, we infused Ang II to enhance cellular damage and in fact, cfDNA, potential TLR9 ligands, levels increased in Ang II–infused animals. A previous study suggested different roles of TLR9 activation according to the concentration of its ligand.[42] The difference in levels of TLR9 ligands attributable to the use of different mouse models might be one of the reasons for the discrepancy. Also, in the study by Koulis et al, total cholesterol was higher in *Tlr9*$^{-/-}$*Apoe*$^{-/-}$ mice with an unknown mechanism; however, in the present study, there was no difference in plasma lipid levels between *Apoe*$^{-/-}$ mice and *Tlr9*$^{-/-}$*Apoe*$^{-/-}$ mice. This might

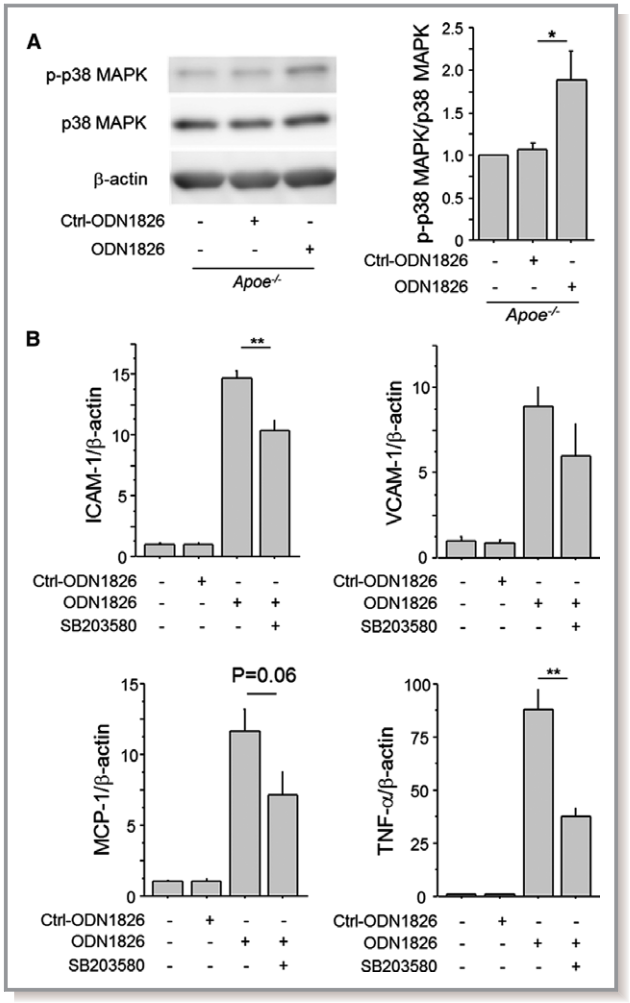

Figure 8. Inhibition of p38 MAPK suppresses TLR9-induced macrophage activation. **A**, Ligation of ODN1826 (100 nmol/L) to TLR9 activated the MAPK pathway determined by the phosphorylation of p38 MAPK in *Apoe*$^{-/-}$ macrophages (n=4–5). Comparison between ODN1826-treated group and Ctrl-ODN1826–treated group was performed with Mann–Whitney *U* test. **B**, The p38 MAPK inhibitor, SB203580 (10 μmol/L), abrogated the expression of inflammatory molecules, such as VCAM-1, ICAM-1, MCP-1, and TNF-α, which are induced by TLR9 activation with ODN1826 (100 nmol/L) in *Apoe*$^{-/-}$ macrophages (n=6). Effects of SB203580 in ODN1826-treated macrophages were analyzed with Mann–Whitney *U* test. **P*<0.05 and ***P*<0.01. All values are mean±SEM. ICAM-1 indicates intercellular cell adhesion molecule-1; MAPK, mitogen-activated protein kinase; MCP-1, monocyte chemoattractant protein-1; qPCR, quantitative real-time polymerase chain reaction; TLR9, Toll-like receptor 9; TNF- α, tumor necrosis factor-α; VCAM-1, vascular cell adhesion molecule-1.

Table 4. Patients' Characteristics

	N=39
Age, y	70.0±1.8
Male sex	25 (64)
Hypertension	30 (77)
Dyslipidemia	23 (59)
Diabetes mellitus	13 (33)
Current smoking	17 (44)
Obesity (BMI >25)	12 (31)
Family history of CAD	8 (21)
OMI	2 (5)
STEMI/NSTEMI	29/10 (74/26)
Multivessel disease	21 (54)
Total cholesterol, mg/dL	168.6±5.0
LDL cholesterol, mg/dL	98.3±4.4
HDL cholesterol, mg/dL	43.9±2.4
Triglyceride, mg/dL	87.3±9.1
HbA_{1c}, %	6.4±0.2
Glucose, mg/dL	172.7±11.2
CK on admission, IU/mL	350.6±120.0
Peak CK, IU/mL	2140.2±311.5
CCB	16 (41)
RAS-I	12 (31)
β-blocker	2 (5)
Statin	7 (18)
Anti-DM	6 (15)
Insulin	2 (5)

All values are n (%) or mean±SEM. BMI, body mass index; CAD, coronary artery disease; CCB, calcium channel blocker; CK, creatine kinase; DM, diabetes mellitus; HbA_{1c}, hemoglobin A_{1c}; HDL, high-density lipoprotein; LDL, low-density lipoprotein; NSTEMI, non–ST-segment elevation myocardial infarction; OMI, old myocardial infarction; RAS-I, renin–angiotensin system inhibitor, STEMI, ST-segment elevation myocardial infarction.

contribute to the discrepancy. Similar to that study, in this study, *Tlr9*$^{-/-}$*Apoe*$^{-/-}$ mice had larger atherosclerotic lesions compared with *Apoe*$^{-/-}$ mice under vehicle infusion condition, although blood lipid levels were equivalent between 2 strains of mice (Figure S4 and Table S2). Thus, we speculate that the role of TLR9 in the development of vascular inflammation and atherogenesis may differ according to the disease conditions. However, in addition to in vivo studies, in our present study, we demonstrated a proinflammatory role of TLR9 in macrophage activation, which supports our in vivo data. These results suggest the proatherogenic roles of cfDNA-TLR9 signaling, at least in an Ang II–infused condition. Further studies are needed to elucidate the contribution of cfDNA-TLR9 signaling to atherogenesis and its mechanism.

Finally, in this study, we examined the association between plasma cfDNA level and plaque characteristics determined by OCT in patients with acute MI who underwent percutaneous coronary intervention. OCT is a high-resolution imaging

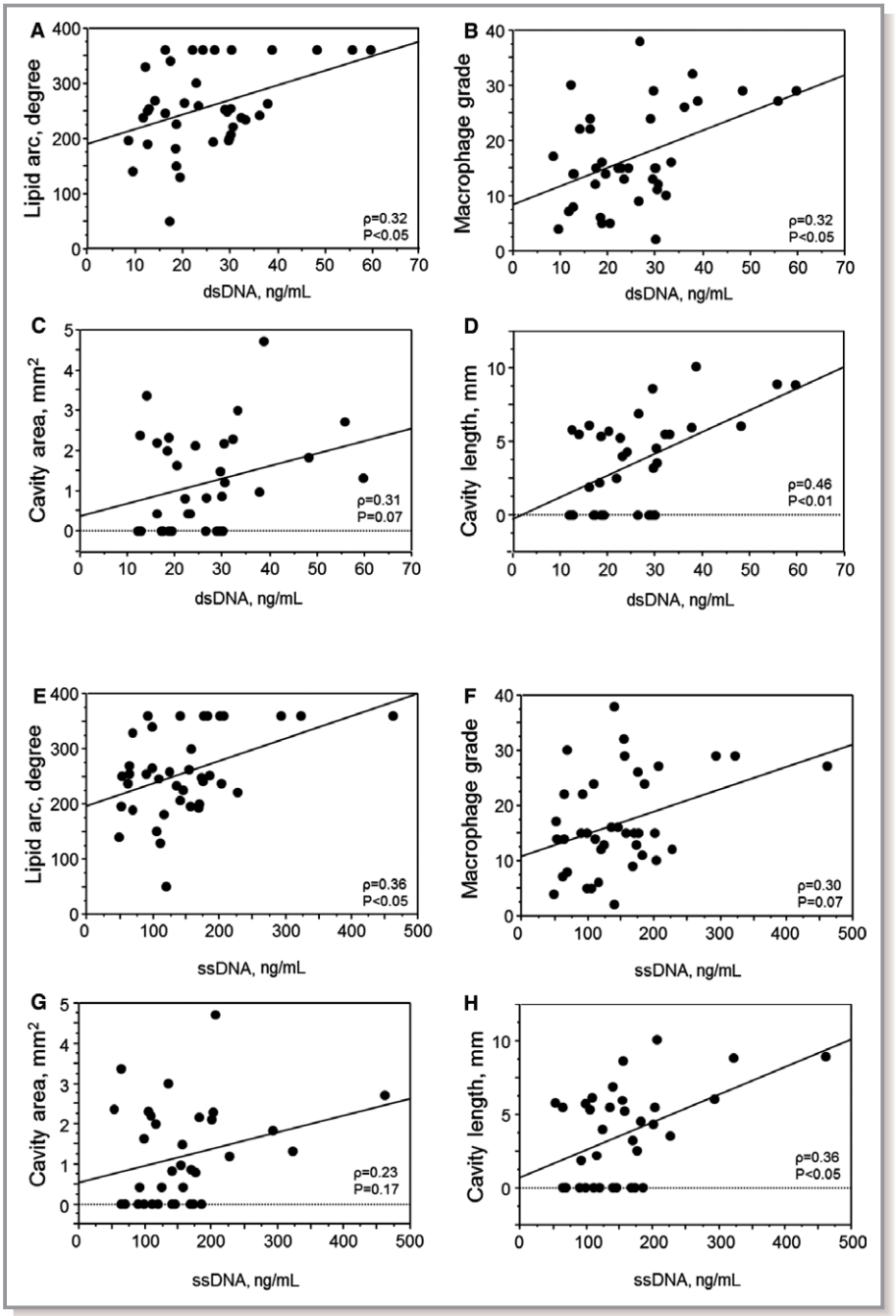

Figure 9. Plasma cfDNA levels positively correlate with inflammatory features of coronary atherosclerosis. Plasma dsDNA or ssDNA level in the target coronary artery positively correlated with inflammatory features of coronary atherosclerosis, such as lipid arc (**A** and **E**) and macrophage grade (**B** and **F**) determined by OCT (n=39). Plasma dsDNA or ssDNA level in the target coronary artery also showed a positive correlation with cavity area (**C** and **G**) or length (**D** and **H**) in ruptured coronary artery plaques (n=35). Univariate analysis between plaque characteristics and plasma dsDNA or ssDNA level was performed using Spearman's rank correlation coefficient. cfDNA indicates cell-free DNA; dsDNA, double-stranded DNA; OCT, optical coherence tomography; ssDNA, single-stranded DNA.

technique for plaque characterization,[29] and allows us to assess the features of vulnerable plaques, which are associated with the inflammatory process in the vasculature.[43] A previous study showed that patients with severe coronary artery disease as assessed by coronary computed tomographic angiography have higher plasma dsDNA level,

suggesting inflammatory properties of released DNA fragments.[44] In this study, we further demonstrated that the plasma level of cfDNA collected from the target vessel in acute MI patients positively correlated with lipid arc, macrophage content, and ruptured cavity length/area, all of which are associated with plaque inflammation. Furthermore, a previous study demonstrated the expression of TLR9 in atherosclerotic lesions in humans.[10] Therefore, the results of our clinical study suggested that cfDNA-TLR9 signaling contributes to the development of vascular inflammation in humans, at least partially. Recent studies demonstrated that other DNA sensors may contribute to the pathophysiology of various inflammatory diseases. Therefore, an inflammatory process mediated by other DNA sensors may also be involved in the development of vascular inflammation in the coronary artery. Further studies are required to elucidate the role of DNA sensors such as TLR9 in atherogenesis.

Recent studies have suggested that damage-associated molecular patterns contribute to the development of chronic inflammatory diseases as endogenous ligands that activate the innate immune system.[5] The present study demonstrated that TLR9, originally known as a sensor for exogenous DNA fragments, contributes to proinflammatory activation of macrophages and the development of vascular inflammation and atherosclerosis in *Apoe*$^{-/-}$ mice that receive Ang II infusion. In addition, the results of our clinical study suggested that cfDNA positively correlates with the features of plaque inflammation in patients with acute MI. Thus, the cfDNA-TLR9 axis participates in the pathogenesis of vascular inflammation and atherogenesis and, might be a therapeutic target for atherosclerotic disease.

Acknowledgments

All authors are grateful to E. Uematsu, S. Okamoto (Tokushima Univ.), H. Kato, and Y. Sugawara (Tokyo Univ.) for their expert technical assistance. The authors also thank Dr Yoshihiro Okayama, University Hospital of Tokushima Clinical Trial Center for Developmental Therapeutics, for his significant advice for statistical analyses.

Sources of Funding

This work was partially supported by Japan Society for the Promotion of Science Kakenhi Grants (number 16K09517 to Fukuda, and number 16H05299 and 26248050 to M. Sata), Takeda Science Foundation (Fukuda and M. Sata), SENSHIN Medical Research Foundation (Fukuda), Katsunuma Scholarship (Nishimoto), Public Trust Cardiovascular Research Fund (Nishimoto), the Fugaku Trust for Medical Research (M. Sata), and the Vehicle Racing Commemorative Foundation (M. Sata). The funders had no role in the study design, data collection, and analysis, or preparation of the manuscript.

Disclosures

The Department of Cardio-Diabetes Medicine, Tokushima University Graduate School, is supported in part by unrestricted research grants from Boehringer Ingelheim, Tanabe-Mitsubishi, Kowa, and Actelion. All authors declare that they have no conflict of interest.

References

1. Libby P. Inflammation in atherosclerosis. *Arterioscler Thromb Vasc Biol*. 2012;32:2045–2051.
2. Hansson GK, Libby P, Schonbeck U, Yan ZQ. Innate and adaptive immunity in the pathogenesis of atherosclerosis. *Circ Res*. 2002;91:281–291.
3. Uematsu S, Akira S. Toll-like receptors and innate immunity. *J Mol Med (Berl)*. 2006;84:712–725.
4. Chen GY, Nunez G. Sterile inflammation: sensing and reacting to damage. *Nat Rev Immunol*. 2010;10:826–837.
5. Zheng Y, Gardner SE, Clarke MC. Cell death, damage-associated molecular patterns, and sterile inflammation in cardiovascular disease. *Arterioscler Thromb Vasc Biol*. 2011;31:2781–2786.
6. Bieghs V, Trautwein C. The innate immune response during liver inflammation and metabolic disease. *Trends Immunol*. 2013;34:446–452.
7. Hagerling C, Casbon AJ, Werb Z. Balancing the innate immune system in tumor development. *Trends Cell Biol*. 2015;25:214–220.
8. Rifkin IR, Leadbetter EA, Busconi L, Viglianti G, Marshak-Rothstein A. Toll-like receptors, endogenous ligands, and systemic autoimmune disease. *Immunol Rev*. 2005;204:27–42.
9. Cole JE, Kassiteridi C, Monaco C. Toll-like receptors in atherosclerosis: a "Pandora's box" of advances and controversies. *Trends Pharmacol Sci*. 2013;34:629–636.
10. Edfeldt K, Swedenborg J, Hansson GK, Yan ZQ. Expression of toll-like receptors in human atherosclerotic lesions: a possible pathway for plaque activation. *Circulation*. 2002;105:1158–1161.
11. Vollmer J. TLR9 in health and disease. *Int Rev Immunol*. 2006;25:155–181.
12. Mogensen TH, Paludan SR, Kilian M, Ostergaard L. Live *Streptococcus pneumoniae*, *Haemophilus influenzae*, and *Neisseria meningitidis* activate the inflammatory response through Toll-like receptors 2, 4, and 9 in species-specific patterns. *J Leukoc Biol*. 2006;80:267–277.
13. Atamaniuk J, Hsiao YY, Mustak M, Bernhard D, Erlacher L, Fodinger M, Tiran B, Stuhlmeier KM. Analysing cell-free plasma DNA and SLE disease activity. *Eur J Clin Invest*. 2011;41:579–583.
14. Barrat FJ, Meeker T, Gregorio J, Chan JH, Uematsu S, Akira S, Chang B, Duramad O, Coffman RL. Nucleic acids of mammalian origin can act as endogenous ligands for Toll-like receptors and may promote systemic lupus erythematosus. *J Exp Med*. 2005;202:1131–1139.
15. Roshan MH, Tambo A, Pace NP. The role of TLR2, TLR4, and TLR9 in the pathogenesis of atherosclerosis. *Int J Inflam*. 2016;2016:1532832.
16. Scharfe-Nugent A, Corr SC, Carpenter SB, Keogh L, Doyle B, Martin C, Fitzgerald KA, Daly S, O'Leary JJ, O'Neill LA. TLR9 provokes inflammation in response to fetal DNA: mechanism for fetal loss in preterm birth and preeclampsia. *J Immunol*. 2012;188:5706–5712.
17. Nishimoto S, Fukuda D, Higashikuni Y, Tanaka K, Hirata Y, Murata C, Kim-Kaneyama JR, Sato F, Bando M, Yagi S, Soeki T, Hayashi T, Imoto I, Sakaue H, Shimabukuro M, Sata M. Obesity-induced DNA released from adipocytes stimulates chronic adipose tissue inflammation and insulin resistance. *Sci Adv*. 2016;2:e1501332.
18. Fukuda D, Aikawa E, Swirski FK, Novobrantseva TI, Kotelianski V, Gorgun CZ, Chudnovskiy A, Yamazaki H, Croce K, Weissleder R, Aster JC, Hotamisligil GS, Yagita H, Aikawa M. Notch ligand delta-like 4 blockade attenuates atherosclerosis and metabolic disorders. *Proc Natl Acad Sci U S A*. 2012;109:E1868–E1877.
19. Isner JM, Kearney M, Bortman S, Passeri J. Apoptosis in human atherosclerosis and restenosis. *Circulation*. 1995;91:2703–2711.
20. Littlewood TD, Bennett MR. Apoptotic cell death in atherosclerosis. *Curr Opin Lipidol*. 2003;14:469–475.
21. Martinet W, Schrijvers DM, De Meyer GR. Necrotic cell death in atherosclerosis. *Basic Res Cardiol*. 2011;106:749–760.
22. Tabas I. Macrophage death and defective inflammation resolution in atherosclerosis. *Nat Rev Immunol*. 2010;10:36–46.
23. Daugherty A, Cassis L. Angiotensin II-mediated development of vascular diseases. *Trends Cardiovasc Med*. 2004;14:117–120.

24. Herbert KE, Mistry Y, Hastings R, Poolman T, Niklason L, Williams B. Angiotensin II-mediated oxidative DNA damage accelerates cellular senescence in cultured human vascular smooth muscle cells via telomere-dependent and independent pathways. *Circ Res*. 2008;102:201–208.
25. Fukuda D, Sata M, Ishizaka N, Nagai R. Critical role of bone marrow angiotensin II type 1 receptor in the pathogenesis of atherosclerosis in apolipoprotein E deficient mice. *Arterioscler Thromb Vasc Biol*. 2008;28:90–96.
26. Daugherty A, Manning MW, Cassis LA. Antagonism of AT2 receptors augments angiotensin II-induced abdominal aortic aneurysms and atherosclerosis. *Br J Pharmacol*. 2001;134:865–870.
27. Nishiguchi T, Tanaka A, Taruya A, Emori H, Ozaki Y, Orii M, Shiono Y, Shimamura K, Kameyama T, Yamano T, Yamaguchi T, Matsuo Y, Ino Y, Kubo T, Hozumi T, Hayashi Y, Akasaka T. Local matrix metalloproteinase 9 level determines early clinical presentation of ST-segment-elevation myocardial infarction. *Arterioscler Thromb Vasc Biol*. 2016;36:2460–2467.
28. Komukai K, Kubo T, Kitabata H, Matsuo Y, Ozaki Y, Takarada S, Okumoto Y, Shiono Y, Orii M, Shimamura K, Ueno S, Yamano T, Tanimoto T, Ino Y, Yamaguchi T, Kumiko H, Tanaka A, Imanishi T, Akagi H, Akasaka T. Effect of atorvastatin therapy on fibrous cap thickness in coronary atherosclerotic plaque as assessed by optical coherence tomography: the EASY-FIT study. *J Am Coll Cardiol*. 2014;64:2207–2217.
29. Tearney GJ, Regar E, Akasaka T, Adriaenssens T, Barlis P, Bezerra HG, Bouma B, Bruining N, Cho JM, Chowdhary S, Costa MA, de Silva R, Dijkstra J, Di Mario C, Dudek D, Falk E, Feldman MD, Fitzgerald P, Garcia-Garcia HM, Gonzalo N, Granada JF, Guagliumi G, Holm NR, Honda Y, Ikeno F, Kawasaki M, Kochman J, Koltowski L, Kubo T, Kume T, Kyono H, Lam CC, Lamouche G, Lee DP, Leon MB, Maehara A, Manfrini O, Mintz GS, Mizuno K, Morel MA, Nadkarni S, Okura H, Otake H, Pietrasik A, Prati F, Raber L, Radu MD, Rieber J, Riga M, Rollins A, Rosenberg M, Sirbu V, Serruys PW, Shimada K, Shinke T, Shite J, Siegel E, Sonoda S, Suter M, Takarada S, Tanaka A, Terashima M, Thim T, Uemura S, Ughi GJ, van Beusekom HM, van der Steen AF, van Es GA, van Soest G, Virmani R, Waxman S, Weissman NJ, Weisz G. Consensus standards for acquisition, measurement, and reporting of intravascular optical coherence tomography studies: a report from the International Working Group for Intravascular Optical Coherence Tomography Standardization and Validation. *J Am Coll Cardiol*. 2012;59:1058–1072.
30. Ino Y, Kubo T, Tanaka A, Kuroi A, Tsujioka H, Ikejima H, Okouchi K, Kashiwagi M, Takarada S, Kitabata H, Tanimoto T, Komukai K, Ishibashi K, Kimura K, Hirata K, Mizukoshi M, Imanishi T, Akasaka T. Difference of culprit lesion morphologies between ST-segment elevation myocardial infarction and non–ST-segment elevation acute coronary syndrome: an optical coherence tomography study. *JACC Cardiovasc Interv*. 2011;4:76–82.
31. Li H, Sun B. Toll-like receptor 4 in atherosclerosis. *J Cell Mol Med*. 2007;11:88–95.
32. Michelsen KS, Wong MH, Shah PK, Zhang W, Yano J, Doherty TM, Akira S, Rajavashisth TB, Arditi M. Lack of Toll-like receptor 4 or myeloid differentiation factor 88 reduces atherosclerosis and alters plaque phenotype in mice deficient in apolipoprotein E. *Proc Natl Acad Sci U S A*. 2004;101:10679–10684.
33. Mullick AE, Tobias PS, Curtiss LK. Modulation of atherosclerosis in mice by Toll-like receptor 2. *J Clin Invest*. 2005;115:3149–3156.
34. Moore KJ, Tabas I. Macrophages in the pathogenesis of atherosclerosis. *Cell*. 2011;145:341–355.
35. Morishige K, Kacher DF, Libby P, Josephson L, Ganz P, Weissleder R, Aikawa M. High-resolution magnetic resonance imaging enhanced with superparamagnetic nanoparticles measures macrophage burden in atherosclerosis. *Circulation*. 2010;122:1707–1715.
36. Kaminska B. MAPK signalling pathways as molecular targets for anti-inflammatory therapy—from molecular mechanisms to therapeutic benefits. *Biochim Biophys Acta*. 2005;1754:253–262.
37. Muslin AJ. MAPK signalling in cardiovascular health and disease: molecular mechanisms and therapeutic targets. *Clin Sci (Lond)*. 2008;115:203–218.
38. Shi H, Yu CQ, Xie LS, Wang ZJ, Zhang P, Zheng LY. Activation of TLR9-dependent p38MAPK pathway in the pathogenesis of primary Sjogren's syndrome in NOD/Ltj mouse. *J Oral Pathol Med*. 2014;43:785–791.
39. Krogmann AO, Lusebrink E, Steinmetz M, Asdonk T, Lahrmann C, Lutjohann D, Nickenig G, Zimmer S. Proinflammatory stimulation of Toll-like receptor 9 with high dose CpG ODN 1826 impairs endothelial regeneration and promotes atherosclerosis in mice. *PLoS One*. 2016;11:e0146326.
40. Ma C, Ouyang Q, Huang Z, Chen X, Lin Y, Hu W, Lin L. Toll-like receptor 9 inactivation alleviated atherosclerotic progression and inhibited macrophage polarized to M1 phenotype in ApoE$^{-/-}$ mice. *Dis Markers*. 2015;2015:909572.
41. Koulis C, Chen YC, Hausding C, Ahrens I, Kyaw TS, Tay C, Allen T, Jandeleit-Dahm K, Sweet MJ, Akira S, Bobik A, Peter K, Agrotis A. Protective role for Toll-like receptor-9 in the development of atherosclerosis in apolipoprotein E–deficient mice. *Arterioscler Thromb Vasc Biol*. 2014;34:516–525.
42. Wu J, Cui H, Dick AD, Liu L. TLR9 agonist regulates angiogenesis and inhibits corneal neovascularization. *Am J Pathol*. 2014;184:1900–1910.
43. Hansson GK, Libby P, Tabas I. Inflammation and plaque vulnerability. *J Intern Med*. 2015;278:483–493.
44. Borissoff JI, Joosen IA, Versteylen MO, Brill A, Fuchs TA, Savchenko AS, Gallant M, Martinod K, Ten Cate H, Hofstra L, Crijns HJ, Wagner DD, Kietselaer B. Elevated levels of circulating DNA and chromatin are independently associated with severe coronary atherosclerosis and a prothrombotic state. *Arterioscler Thromb Vasc Biol*. 2013;33:2032–2040.

Supplemental Material

Table S1. Primer sequences.

	Forward	Reverse
F4/80	5’- TGCATCTAGCAATGGACAGC -3’	5’- GCCTTCTGGATCCATTTGAA -3’
ICAM-1	5’- TTCACACTGAATGCCAGCTC -3’	5’- GTCTGCTGAGACCCCTCTTG -3’
MCP-1	5'-CCACTCACCTGCTGCTACTCAT-3’	5'-TGGTGATCCTCTTGTAGCTCTCC-3’
TLR9	5'-ATGGACGGGAACTGCTACTACA-3’	5'-GACCTTGGAACCAGGAAGAGTT-3’
TNF-α	5'-ACCCTCACACTCAGATCATCTTC-3’	5'-TGGTGGTTTGCTACGACGT-3’
VCAM-1	5'-GCCCATCCTCTGTGACTCAT-3’	5'-AGGCCACAGGTATTTTGTCG-3’
β-actin	5'-CCTGAGCGCAAGTACTCTGTGT-3’	5'-GCTGATCCACATCTGCTGGAA-3’

Table S2. Effect of genetic deletion of TLR9 on metabolic parameters in vehicle infused mice.

	Apoe$^{-/-}$	*Tlr9*$^{-/-}$*Apoe*$^{-/-}$	*P*-value
Body weight, g	31.7±0.8	31.8±1.1	0.72
Heart rate, bpm	750±5	725±12	0.05
Systolic blood pressure, mmHg	100.6±2.6	98.0±2.2	0.56
Diastolic blood pressure, mmHg	64.7±1.9	58.6±2.3	0.05
Total choletesterol, mg/dl	1034.9±80.4	1193.1±135.4	0.29
Triglyceride, mg/dl	140.9±10.9	150.0±23.1	0.71
HDL cholesterol, mg/dl	20.6±1.5	20.1±2.4	0.86

All values are mean ± SEM. HDL; high-density lipoprotein

Figure S1. Effect of genetic deletion of TLR9 on abdominal aortic aneurysm formation and survival curve.

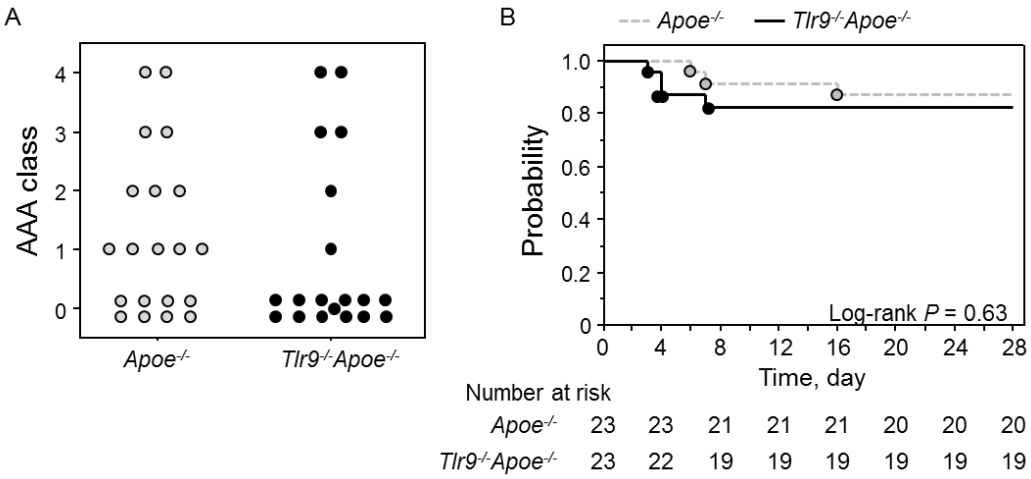

Genetic deletion of TLR9 did not affect the severity of abdominal aortic aneurysm (**A**) and survival curve **(B**) between *Apoe*$^{-/-}$ mice and *Tlr9*$^{-/-}$*Apoe*$^{-/-}$ mice. The severity of abdominal aortic aneurysm and survival curve between the two strains were analyzed by Mann-Whitney U test and Kaplan-Meier method with log-rank test, respectively.

Figure S2. iODN2088, a specific antagonist to TLR9, inhibits TLR9 activation.

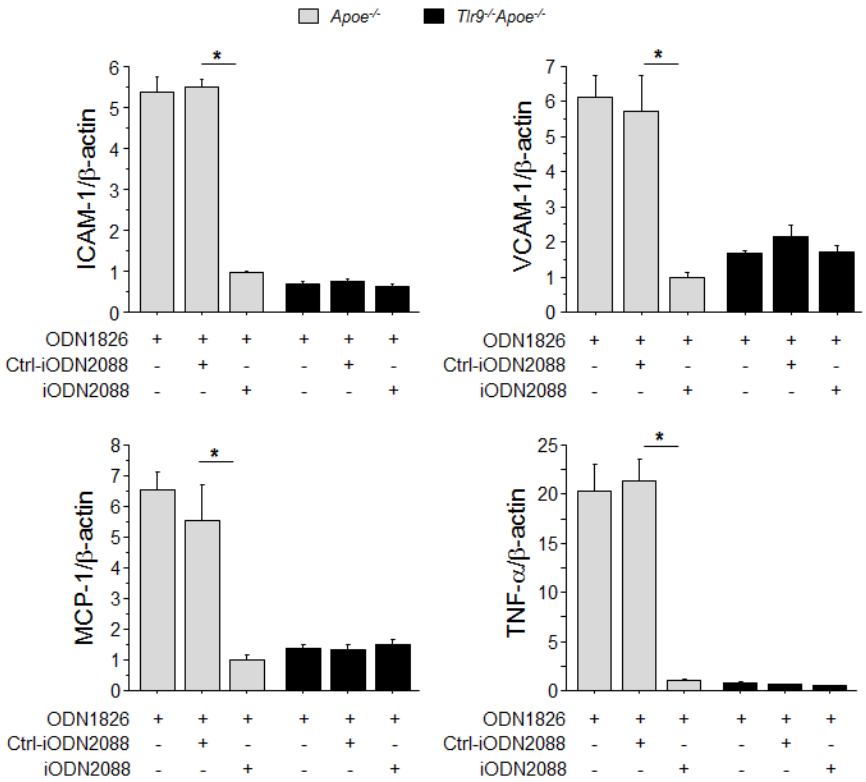

qPCR analysis demonstrated that iODN2088, an inhibitory oligonucleotide for TLR9, blocked inflammatory molecule expression induced by ODN1826. *$P < 0.05$. All comparisons between iODN2088-treated group and Ctrl-iODN-treated group were performed with Mann-Whitney U test. All values are mean ± SEM.

Figure S3. TLR9 ligation promotes p38 MAPK activation in *Apoe*$^{-/-}$ macrophages.

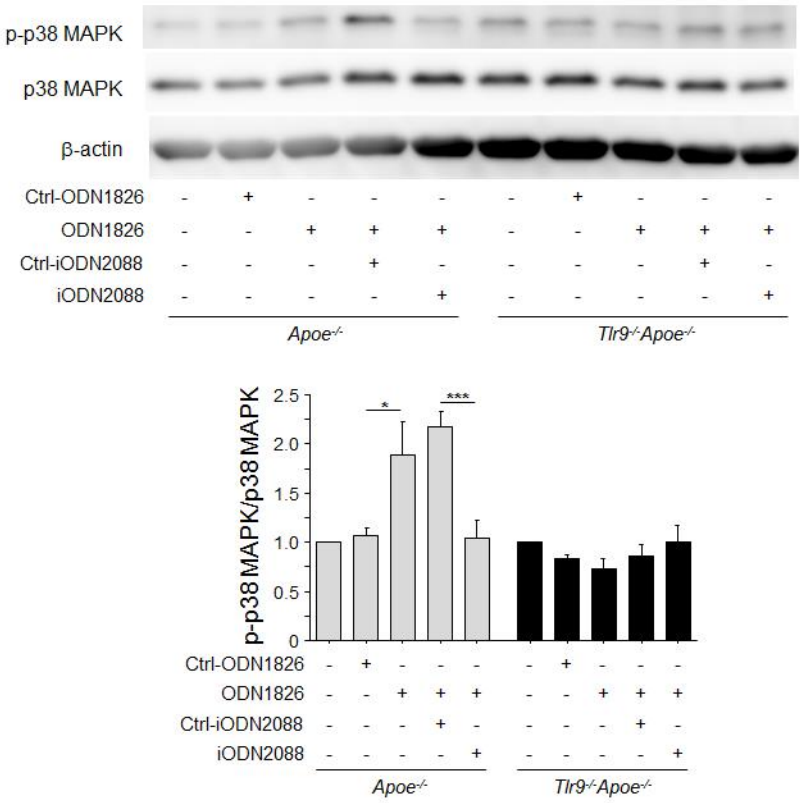

Western blotting analysis showed that ODN1826 increased the phosphorylation of p38 MAPK in *Apoe*$^{-/-}$ macrophages, which was blocked in the presence of iODN2088. Both ODN1826 and iODN2088 did not have any effect in *Tlr9*$^{-/-}$*Apoe*$^{-/-}$ mice. **P*<0.05, and ****P*<0.001. Comparison between ODN1826-treated group and Ctrl-ODN1826-treated group and comparison between iODN2088-treated group and Ctrl-iODN-treated group were performed with Mann-Whitney U test. All values are mean ± SEM.

Figure S4. *Tlr9*$^{-/-}$*Apoe*$^{-/-}$ mice had larger atherosclerotic lesions compared with *Apoe*$^{-/-}$ mice under vehicle infusion condition.

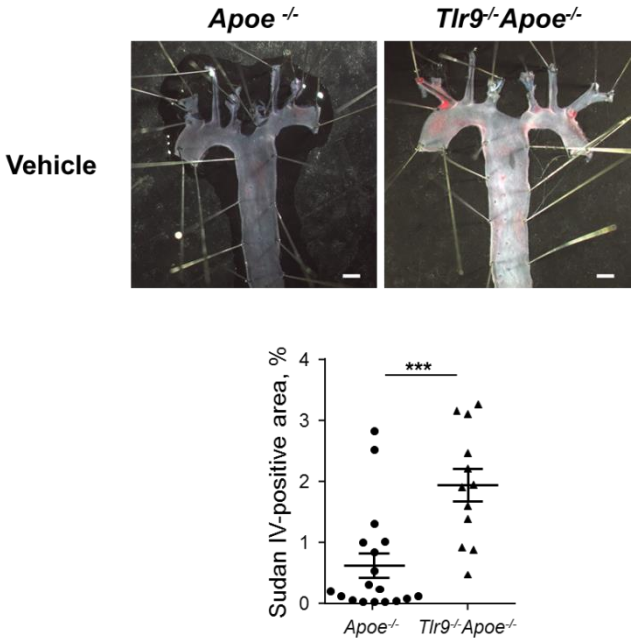

Genetic deletion of TLR9 promoted atherosclerotic lesion development in vehicle-infused *Apoe*$^{-/-}$ mice (n = 12-18). Scale bar; 1 mm. ***P<0.001. Comparison between *Tlr9*$^{-/-}$*Apoe*$^{-/-}$ mice and *Apoe*$^{-/-}$ mice was performed with Mann-Whitney U test. All values are mean ± SEM.